UC Berkeley
Recent Work

Title

Macroscopic Relations of Urban Traffic Variables: An Analysis of Instability

Permalink

https://escholarship.org/uc/item/7qd590bv

Authors

Daganzo, Carlos F.
Gayah, Vikash V.
Gonzales, Eric J.

Publication Date

2010-05-01

Macroscopic Relations of Urban Traffic Variables:
An Analysis of Instability

Carlos F. Daganzo, Vikash V. Gayah and Eric J. Gonzales

WORKING PAPER
UCB-ITS-VWP-2010-4

May 2010

Macroscopic Relations of Urban Traffic Variables: An Analysis of Instability

Carlos F. Daganzo, Vikash V. Gayah and Eric J. Gonzales

UC Berkeley Center for Future Urban Transport,
A Volvo Center of Excellence

May 18, 2010

Abstract

Recent experimental work has shown that the average flow and average density within certain urban networks are related by a unique, reproducible curve known as the Macroscopic Fundamental Diagram (MFD). For networks consisting of a single route this MFD can be predicted analytically; but when the networks consist of multiple overlapping routes experience shows that the flows observed in congestion for a given density are less than those one would predict if the routes were homogeneously congested and did not overlap. These types of networks also tend to jam at densities that are only a fraction of their routes' average jam density.

This paper provides an explanation for this phenomena. It shows that, even for perfectly homogeneous networks with spatially uniform travel patterns, symmetric equilibrium patterns with equal flows and densities across all links are unstable if the average network density is sufficiently high. Instead, the stable equilibrium patterns are asymmetric. For this reason the networks jam at lower densities and exhibit lower flows than one would predict if traffic was evenly distributed.

Analysis of small idealized networks that can be treated as simple dynamical systems shows that these networks undergo a bifurcation at a network-specific critical density such that for lower densities the MFDs have predictably high flows and are univalued, and for higher densities the order breaks down. Simulations show that this bifurcation also manifests itself in large symmetric networks. In this case though, the bifurcation is more pernicious: once the network density exceeds the critical value, the stable state is one of complete gridlock with zero flow. It is therefore important to ensure in real-world applications that a network's density never be allowed to approach this critical value. Fortunately, analysis shows that the bifurcation's critical density increases considerably if the network is redundant and (some of the) drivers choose their routes adaptively in response to traffic conditions.

1   Introduction

The first known theoretical proposal of a unimodal relation between average flow and average density in a network appears to have been made in Godfrey (1969). This idea was later reintroduced in Herman and Ardekani (1988) as a refinement to the two-fluid model of Herman and Prigogine (1979), and then reintroduced once again in Daganzo (2005) as part of an urban traffic dynamics model. But the idea was not tested experimentally in the field until quite recently when advances in ITS supplied the requisite urban-scale data (Geroliminis and Daganzo, 2008). The experiments and simulations in this reference strongly suggest that at least in some instances average flow and density are indeed related by a reproducible curve, which has been come to be known as the 'Macroscopic Fundamental Diagram' (MFD).

Some have argued that this kind of order should, in fact, be expected. For example, Daganzo (2005) proposes that a well-defined relationship between flow and density must arise under time-invariant conditions if a network is 'uniformly loaded' in space so that all of its links are similarly congested. It has also been shown that an MFD must arise for single-route networks with a fixed number of vehicles in circulation (i.e., periodic boundary conditions and no turns) if vehicles obey the kinematic wave theory of traffic flow; see Daganzo and Geroliminis (2008). This reference also gives explicit formulae for the single-route MFD in terms of the route's intersection control patterns, the length of its links and their individual fundamental diagrams (FD's). The reference also posits that this MFD formula should apply to any network of crisscrossing routes if the routes are alike and the numbers of vehicles in these routes are both similar and roughly constant over time. These conditions could be expected to hold for homogeneous, redundant networks with slow-changing demand because network redundancy allows drivers to choose routes adaptively—and, since routes are similar, the densities on each route should then be similar. This would imply that turns into and out of each route are steady and balanced.

Yet, when Geroliminis and Daganzo (2008) apply the single-route MFD formula to networks that approximately meet these homogeneity conditions the predicted flows over-estimate those observed for high network densities. This phenomenon has also been noted in Gonzales et al. (2009) and Mazloumian et al. (2009). The latter attributed the under-prediction to stochastic variations in link densities due to the granularity of the problem.

To look at this issue more deeply, this paper considers the most favorable scenario possible for the MFD: one with perfect spatial homogeneity, time independence and no granularity. It is shown with the simplest type of network sharing these characteristics that if there is any amount of turning, no matter how well balanced, the MFD undergoes a bifurcation and may become multi-valued for high densities. This phenomenon should not be a total surprise because some networks with multiple route choices are known to exhibit multiple capacity states; and this strongly suggests that multivaluedness, and even chaos, could arise in severely congested networks; see Daganzo (1998). What is perhaps surprising is that multiple capacity states arise in the simplest, most symmetric networks.

By analyzing networks of varying levels of realism, this paper shows that multiple values are to be expected, that network dynamics are inherently unstable, and that these two features are a main cause for the low flows observed for high densities and the networks' propensity to jam. The paper also shows that the undesirable effects diminish with increasing driver adaptation to real-time traffic conditions; that the theoretical single-route MFD is an upper bound to the flow-density states that arise in simulations; and that the density at which a multi-route network jams is always considerably smaller that its theoretical jam density.

Section 2 below describes the network idealizations used in this paper. Section 3 examines analytically the simplest of these. Then, Section 4 shows with simulations that more realistic network representations exhibit the same phenomena, and Section 5 investigates the effect of driver

adaptation.

2 A Rectangular Grid and Two Possible Idealizations

The network is a homogeneous rectangular grid of one-directional roads with alternating direction-ality; see Figure 1a. All the links in each family of parallel roads i, where $i = 1$ or 2, have the same length, L_i, and obey the same fundamental diagram (FD), $Q_i(k)$, independent of directionality. The FD's are assumed to be triangular with capacity q_{ic}, jam density k_{ij}, free flow speed v_i and backward wave speed $w_i < v_i$ (see Figure 1b) because this is realistic and simple; but the qualitative results of this paper do not hinge on this specific shape. The translational symmetry of the links also extends to the control strategy for each intersection.
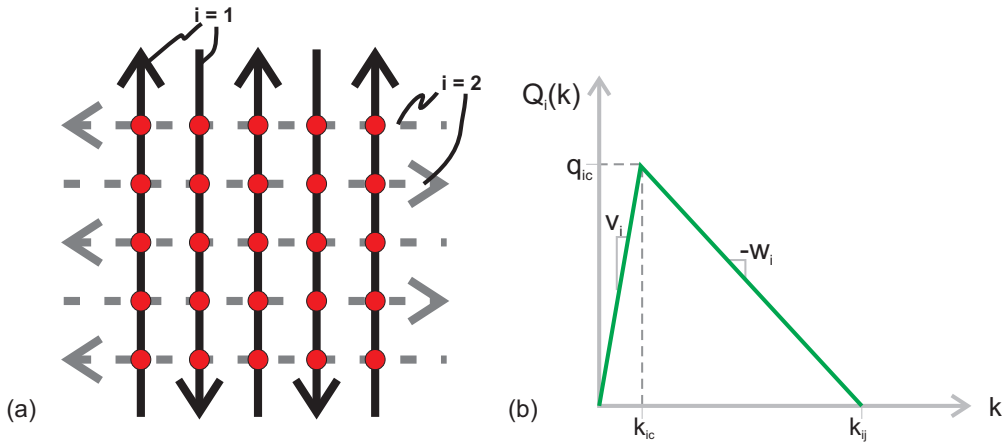

Figure 1. (a) An Idealized City Network; (b) Fundamental Diagram of Individual Links (Symmetric Network).

Cars are allowed to make legal turns at intersections, but to maintain a fixed number of cars in the system over time, they are not allowed to enter or exit the links in any other way. In fact, for every car that exits a road at its downstream end, another one is simultaneously inserted at its upstream end. This set up also ensures that cars are conserved in each individual road if no turns are allowed. It is also assumed until Section 5 that drivers do not adapt to traffic conditions and, therefore, turns at intersections are exogenously determined.

2.1 A Two-Ring Idealization

To further simplify analysis, it will be assumed in parts of this paper that the fraction of traffic wishing to turn from one family of roads to the other, denoted P_T, is the same at every intersection at all times. This simplification, which we call 'correlated turns,' ensures that if the link density profile at a moment in time is the same for all the links within each family of roads, it stays the same among links within each family from then on. This type of homogeneity facilitates analysis because the system can then be studied by keeping track of only two links. In fact, a physically equivalent model consists of just two tangent rings where vehicles circulate clockwise and counter-clockwise, switching from one ring (i.e. from one road family) to the other as they pass the point of tangency; see Figure 2a. The shades of grey in this figure correspond to those of Figure 1a. The turning rate is the product of the flow directly upstream of the intersection (as determined by the intersection control law) and P_T.
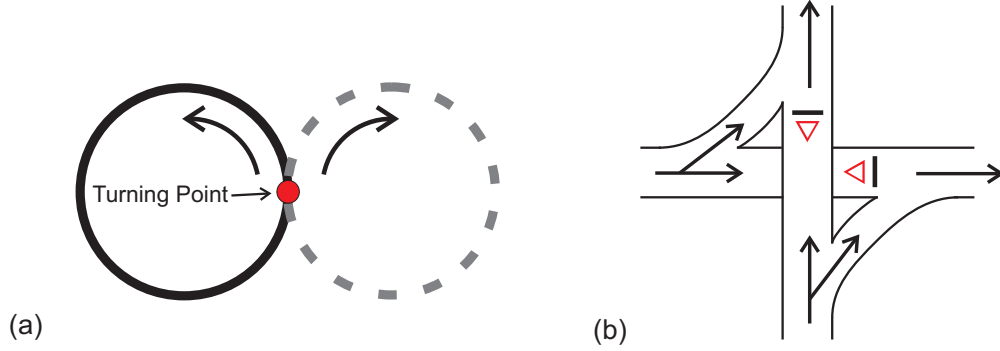
Figure 2. (a) Simplest Model that Describes Network; (b) Intersection Control Strategy

We say that this type of system is in equilibrium (or in an equilibrium state) if the density profiles and turning flows are invariant with time.[1] For this to happen the two turning flows must cancel each other out. We say that an equilibrium is 'stable' if the system returns to equilibrium after any minor perturbations to the equilibrium link density profiles.

2.2 A Two-Bin Idealization and Its Dynamics

The two-ring model is now approximately analyzed for conditions near equilibrium assuming that: (i) intersections are unsignalized and organized as in Figure 2b; and, (ii) turning traffic has priority and can be absorbed by the target link unless that link is jammed.

With unsignalized intersections, a link's density should be fairly homogeneous along its length near equilibrium, so we approximate the flow at its downstream end by:

$$q_i = Q_i(k_i) \tag{1}$$

where k_i is the average density along the link's entire length. This simplification is convenient because it characterizes the state of a link by a single value, its average density, as if it was a memoryless 'bin' instead of a 'ring'. The simplification is not realistic, however, when the system is far from equilibrium and conditions change rapidly with time.

Given these assumptions, the turning flow, $f_i \doteq P_T q_i$, is the following function F_i of the average density:

$$f_i = F_i(k_i) \doteq P_T Q_i(k_i). \tag{2}$$

This equation allows us to enumerate all possible equilibria for different network densities, k_T,

$$k_T = \frac{k_1 L_1 + k_2 L_2}{L_1 + L_2}, \tag{3a}$$

by simply checking the condition: $F_1 = F_2$. An expression similar to (3a) applies for Edie's generalized definition of network flow (Edie, 1965):

$$q_T = \frac{q_1 L_1 + q_2 L_2}{L_1 + L_2}. \tag{3b}$$

The two-bin model can be analyzed with ODE methods. The following equations, combined

---

[1]If intersections are controlled by traffic signals, the equilibrium definition can be used only approximately on time scales that are large compared with the signal cycles.

with (3), describe its dynamics near equilibrium for a fixed P_T:

$$\frac{dk_1}{dt} = \frac{F_2(k_2) - F_1(k_1)}{L_1} \text{ and } \frac{dk_2}{dt} = \frac{F_1(k_1) - F_2(k_2)}{L_2}, \text{ if no ring is jammed;} \tag{4a}$$

$$\frac{dk_1}{dt} = \frac{dk_2}{dt} = 0, \text{ otherwise.} \tag{4b}$$

Equilibrium solutions to ODEs of this type are stable if and only if any perturbation in k_1 from the equilibrium state always causes a perturbation in dk_1/dt of the opposite sign. The reader can verify from (3a) that a perturbation ϵ in k_1 must be accompanied by a perturbation $(L_1/L_2)\epsilon$ in k_2 if k_T is to remain invariant. If these two perturbations are now inserted in (4a) (for an equilibrium where $F_1 = F_2$), one finds that dk_1/dt and $-dk_2/dt$ change by the same amount: $-[(dF_1/dk_1)/L_1 + (dF_2/dk_2)/L_2]\epsilon$. Thus, an equilibrium is stable if:

$$\frac{dF_1/dk_1}{L_1} + \frac{dF_2/dk_2}{L_2} > 0, \text{ and no ring is jammed; or} \tag{5a}$$

$$\frac{dk_1}{dt} = \frac{dk_2}{dt} = 0, \text{ otherwise.} \tag{5b}$$

If the LHS of (5a) is negative the equilibrium is unstable, as any perturbations would grow in magnitude. Determining stability is important because unstable equilibria are self-destructing and cannot be observed: only stable equilibria can form part of an MFD. Therefore, we now explore with the help of this simple model the possible stable equilibrium patterns of a two-bin system with two identical bins. The two-bin idealization is relaxed in Section 4.

3 Two-Bin Model of a Square Grid

Considered here is the special case of a square grid where the two road families are identical in all relevant aspects. Therefore, the subscript 'i' is dropped from the parameter notation. Subscripts must be retained for variables, however.

With this notation the equilibrium conditions are:

$$F_1(k_1) = F_2(k_2) \Leftrightarrow Q(k_1) = Q(k_2) \text{ if } k_1, k_2 \neq k_j; \text{ or} \tag{6a}$$

$$k_1 = k_j \text{ or } k_2 = k_j. \tag{6b}$$

and the stability conditions (5) become:

$$\frac{\partial F_1}{\partial k_1} + \frac{\partial F_2}{\partial k_2} > 0 \Leftrightarrow \frac{\partial Q_1}{\partial k_1} + \frac{\partial Q_2}{\partial k_2} > 0; \text{ or} \tag{7a}$$

$$k_1 = k_j \text{ or } k_2 = k_j. \tag{7b}$$

Note that (6) and (7) are independent of the turning fraction, P_T, for $P_T > 0$.

The average network density and network flow can be expressed similarly:

$$k_T = \frac{k_1 + k_2}{2} \tag{8}$$

$$q_T = \frac{q_1 + q_2}{2} = \frac{Q(k_1) + Q(k_2)}{2}. \tag{9}$$

Equations (6) and (7) are now used to identify all the stable equilibria; and (8) and (9) to

calculate the corresponding points (k_T, q_T) of the MFD. The three frames in Figure 3 show how the former can be done with a simple graphical construction that superimposes plots of either $F(k_1)$ and $F(k_2)$, or $Q(k_1)$ and $Q(k_2)$.
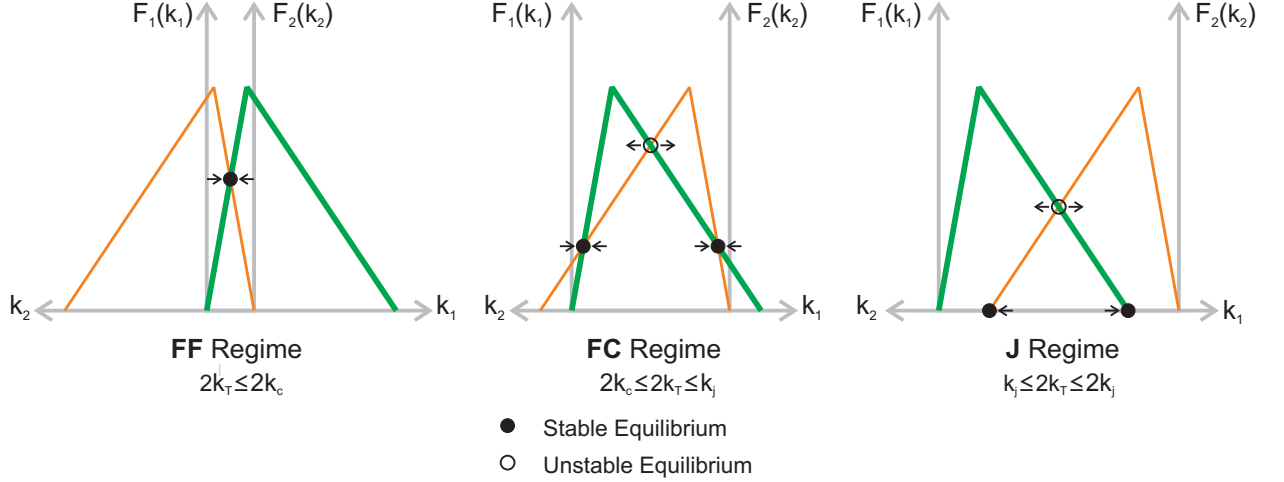

Figure 3. Possible Regimes for Symmetric 2-bin System.

These curves are drawn with the axes for k_1 and k_2 running in opposite directions and the origins separated by $2k_T$ units, so that the two abscissas of any point in between the two vertical axes identify k_1 and k_2, as per (8). Clearly, (6) is then satisfied where the two curves cross, or at the jam point of either curve. The figure shows three different ways in which equilibria can arise depending on whether: (i) $2k_T \leq 2k_c$; (ii) $2k_c \leq 2k_T \leq k_j$; (iii) $k_j \leq 2k_T \leq 2k_j$. Not all equilibria are stable, however: hollow dots represent unstable equilibria because (7a) is violated; i.e., no ring is jammed and the sum of the slopes of the intersecting curves is negative. The solid dots are stable equilibria. Note, their flows are lower than those of the symmetric (unstable) equilibria. The character of the stable equilibria are used to name the three regimes: (i) **F**ree-**F**ree (or FF); (ii) **F**ree-**C**ongested (or FC); (iii) **J**am (or J).

Stability can also be checked from these plots by imagining that a small perturbation sends the equilibrium point either to its left or to its right. If at this new point the dark curve is above the light (i.e. $F_1 > F_2$), then the point will tend to move towards the left, since more flow would be leaving bin 1 than entering it. The arrows in the figure illustrate the direction of these motions. They point away from unstable equilibria, but converge on the stable points.

We can graphically display all states of the system on a phase diagram (see Figure 4a). On the phase diagram, constant values of total density are represented by the gray diagonal lines. Dashed gray lines represent the boundaries between the three different regimes. Solid gray lines with arrows show the direction in which the state moves as per (4). Solid black lines denote the stable equilibria, and the dotted black line the unstable equilibria. Note, that a unique stable equilibrium exists if the system is in the FF regime but a bifurcation arises as k_T is increased and the system moves from the FF to FC regime. For any particular value of k_T in the FC regime, there are two symmetric stable equilibria in which one bin contains more vehicles than the other. This continues for the J regime but now the more congested bin is jammed. Note that in the FC and J regimes, evenly loaded bins are unstable.

The above shows that as the density is increased past the bifurcation, the symmetric equilibrium becomes unstable. And, since the stable equilibria that arise have lower flows than their symmetric (unstable) counterpart, the observed equilibrium flows for high densities should be lower than those that would arise if the two bins were homogeneously congested. Ineed, Figure 4b plots the
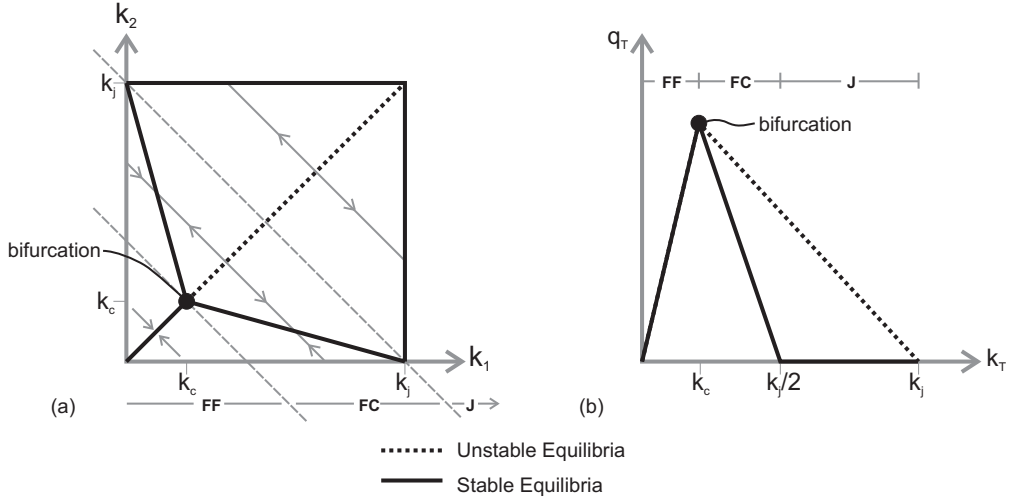
Figure 4. (a) Phase Diagram for Symmetric 2-bin System, (b) MFD for Stable and Unstable Equilibrium States.

average network flow (9) as a function of the average network density (8) for all stable and unstable equilibria. The two stable branches after the bifurcation are superimposed due to the symmetry of the bins. In the FF regime, the MFD of the system is equivalent to the FD of the individual bins. This happens because the number of vehicles is split evenly between the two bins. In the FC and J regimes, however, the theoretical MFD that would be expected from previous work on single routes is unstable. The (stable) MFD is much lower and jams in the range $k_T \in [k_j/2, k_j]$. The jamming of a road network at densities much lower than jam density is a phenomenon that is typically seen in simulations of real networks. Also note that, even though turning causes the phenomenon, the effect is independent of the proportion of turning traffic, P_T. Previous MFD thinking (Daganzo and Geroliminis, 2008) assumed that small amounts of turning traffic would not have a significant effect on the distribution of traffic in a homogeneous network (and therefore no effect on a network's MFD) but this simple system shows that if drivers do not adapt the conjecture is false.

3.1 System Dynamics and Turn Randomness

The dynamics of the two-bin system are now examined when an inflow demand $D_i(t)$ $[veh/hr]$ is continuously inserted in each bin and turning rates are allowed to vary (randomly) with time. With these changes, the dynamic equations become:

$$\frac{\partial k_1(t)}{\partial t} L_1 = D_1(t) - P_T(t)Q(k_1) + P_T(t)Q(2k_T - k_1) \tag{10}$$

$$\frac{\partial k_2(t)}{\partial t} L_2 = D_2(t) + P_T(t)Q(k_1) - P_T(t)Q(2k_T - k_1). \tag{11}$$

This system was then simulated by varying $P_T(t)$ around a given average, $P_T \doteq E_t(P_T(t))$ in a form that would mimic a Bernoulli process. Figure 5 displays the resulting phase paths for many runs with different loading rates and $P_T = 0.5$. This experiment was repeated for other values of P_T with the same qualitative results.

For very slow loading rates, the system has enough time to reach an equilibrium state before new vehicles are added to the network. Therefore, the phase paths bundle together close to the (stable) MFD. Observe too that the system tends to jam at the same density $(k_j/2)$ for each phase
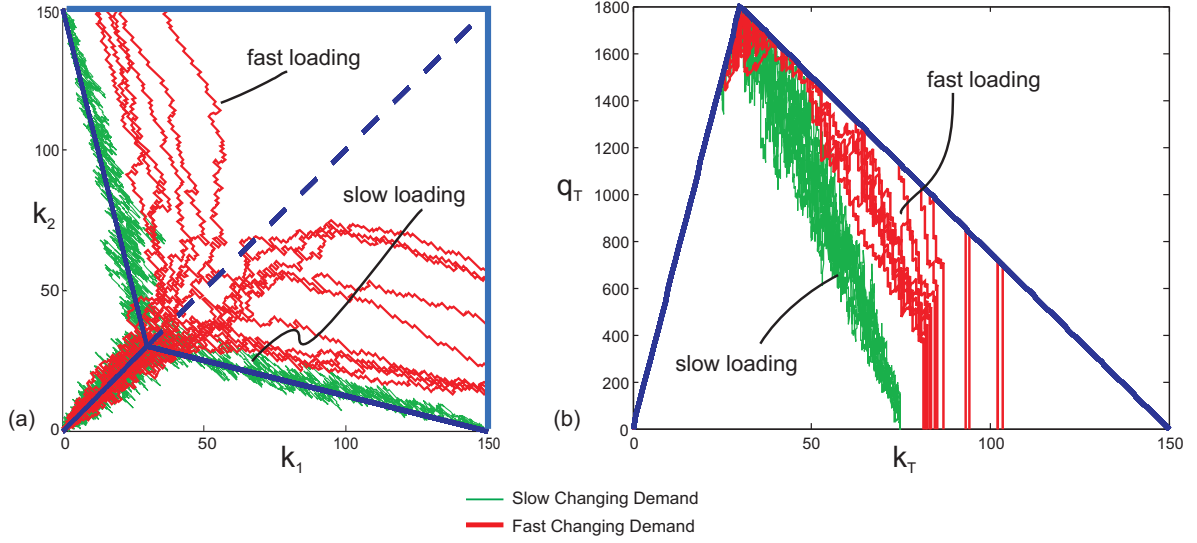
Figure 5. (a) Phase Paths, and (b) Flow-Density Relationships for Different Demand Rates (when $P_T = 0.5$).

path. When the system is loaded quickly, however, the system does not reach an equilibrium before more vehicles are added and as a result phase paths depend on the speed of loading. These phase paths no longer bunch together along a line. These results show that randomness and slow-varying demand do not significantly alter the results of Figure 4. The main new insight is that with fast loading, phase paths can stay close to the unstable equilibria for a while, and then jam at higher densities. All phase paths, however, stay below the theoretical MFD, as expected from theory.

3.2 Network Heterogeneity

The FDs, $Q_i(k)$, of the two road families are now allowed to differ; see Figure 6a. The same logic of Section 3, now using (5) instead of (7), again results in a bifurcation, and unstable equilibria. But now the (stable) MFD is multivalued; see Figure 6b.
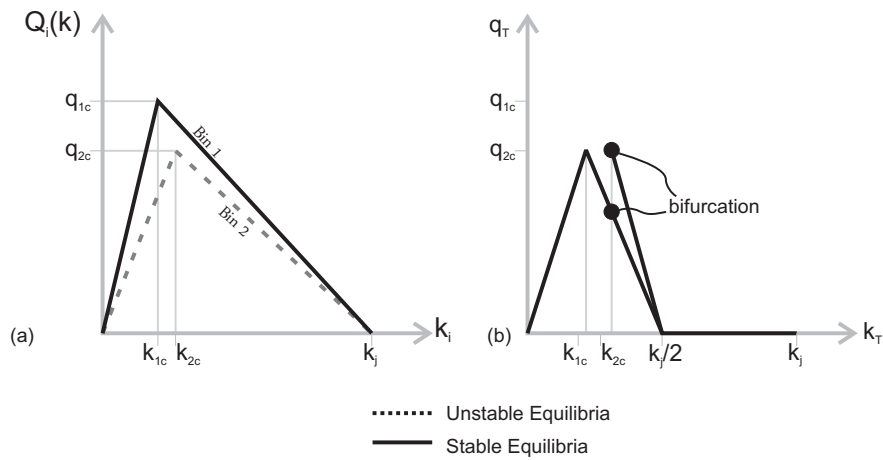

Figure 6. (a) Unique Individual Bin FDs; (b) MFD when Bins are Unique.

4 Tests with Rings and Networks

4.1 Rings

Because the two-bin model of Section 3 is only approximate, its predictions are now compared with those of a two-ring system that captures the spatial dynamics of the link and the boundary conditions of the intersection more realistically. The CA(M) cellular automata model in Daganzo (2006) was used to simulate two homogeneous rings with identical FDs because this model is known to be equivalent to the kinematic wave model of traffic flow[2]. The intersection was still modeled as in Figure 2a, except now turning traffic and through traffic are assumed to have equal priority at the merge locations. Turns were modeled as Bernoulli trials with probability P_T. Vehicles were then slowly added to each ring in equal proportions. An interactive animation can be found at `http://www.ce.berkeley.edu/~daganzo/home.html`. Further details about the simulation can be found in Gayah and Daganzo (2010) (to be submitted).

As in Section 3, the phase paths turn out to be insensitive to P_T, and always close to the (stable) MFD; see Figure 7. This confirms that the analytical two-bin model adequately describes the quasi-equilibrium behavior of a symmetric network with correlated turns.
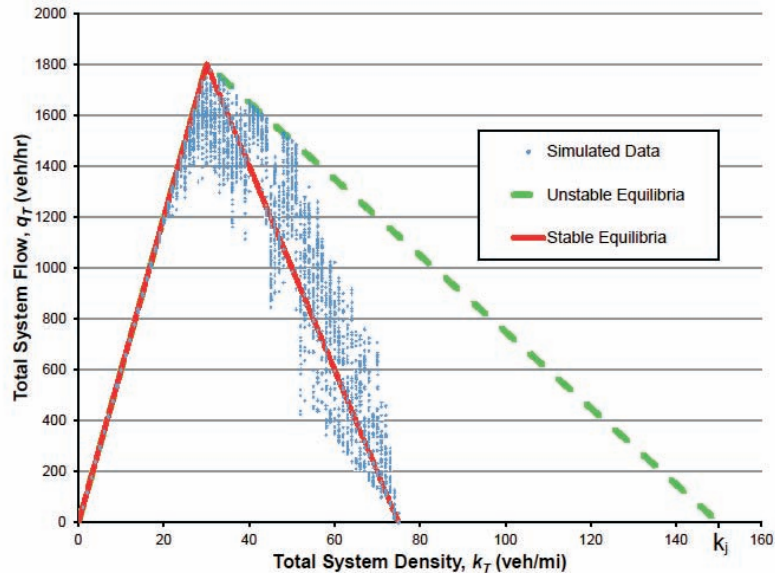

Figure 7. Simulated Flow-Density Relationship for 2-Ring System (with $P_T = 0.05$).

4.2 Networks with Uncorrelated Turns

A network is now studied to examine the effect of uncorrelated turns. With correlated turns, a network can jam in only two ways; i.e., only if all links in a family jam. But with uncorrelated turns, a network can jam in many different ways. To illustrate this effect, Figure 8 shows three gridlocked states arising from three different simulation runs of the network in Figure 1. These runs were started with the same number of vehicles uniformly distributed on the network, and without adding any vehicles to it.

This tendency to jam should not be surprising. If we were to run an infinitely long simulation of a network with only enough vehicles to fill four links, the system would eventually lock itself in

---

[2]This model is also equivalent to the CA(L) cellular automata model originally proposed in Nagel and Schreckenberg (1992), but it is simpler to code.
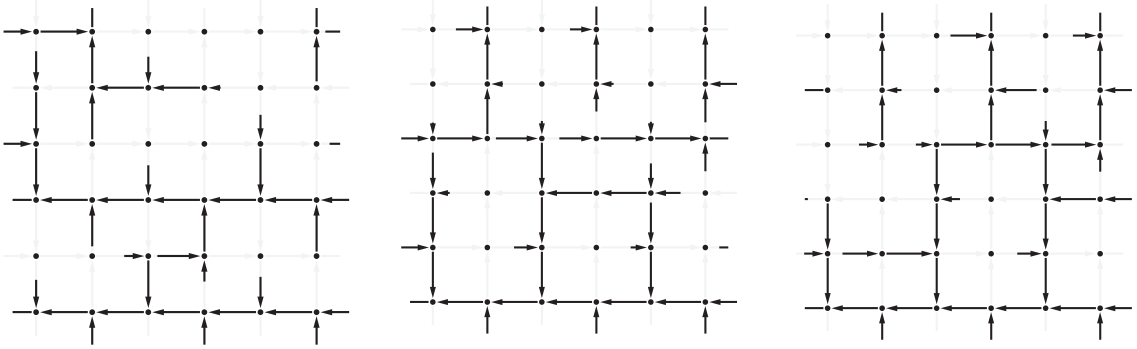
Figure 8. Three Patterns of Jams for a Homogeneous Network (with $k_T = k_j/2$).

a pattern with vehicles wrapping around a block. Clearly, for large networks, virtually the whole range of densities is unstable. Thus, the relevant question for real networks is not whether the system can ever jam, but how long this takes on average. With few vehicles, the probability that all the necessary turns are made to gridlock the system is low, but the network is more likely to jam as the density of vehicles increases. This is illustrated by the simulations in Figure 9. They show, as one might expect, that the time to collapse is astronomically high for small densities ($k < k_j/4$), that there is a narrow range of densities ($k \approx k_j/4$) where the time is comparable with a few hours, and that there is a final range ($k > k_j/4$) where the collapse is rapid. They also show that these ranges are insensitive to the probability of turning, P_T.
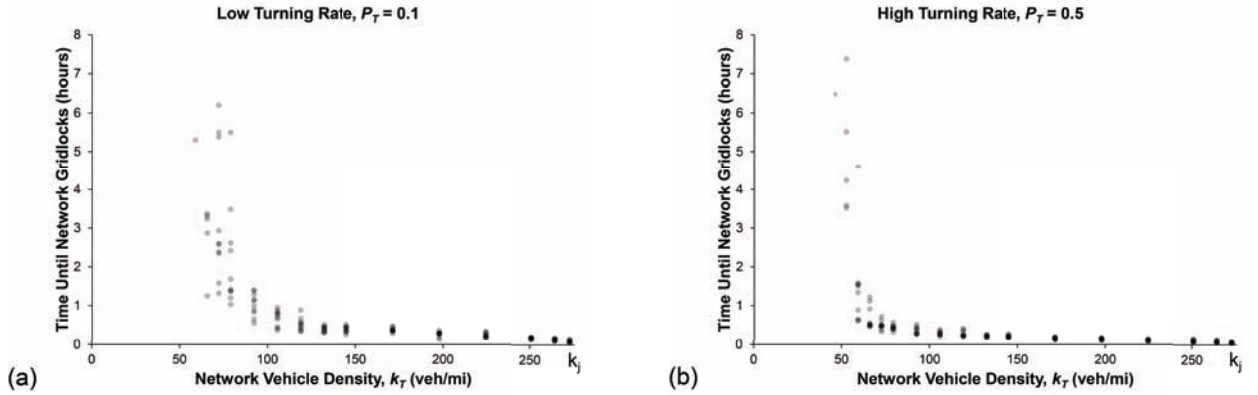

Figure 9. Elapsed Time to Gridlock Starting with Uniformly Distributed Vehicles for (a) $P_T = 0.1$ and (b) $P_T = 0.5$.

The macroscopic flow density data associated with the simulations at each of these vehicle densities are shown in Figure 10. Each gray dot represents a 1 minute aggregation of vehicle density and network flow. Black indicates many overlapping observations. For low vehicle densities, the probability of gridlock is so low that it is not observed even for simulations as long as 50 hours. Flow increases with density in this (practically) stable regime. As vehicle density increases, there is first a narrow metastable range where high flows can be sustained, but only for a few hours, and then an unstable range where the network collapses in less than 1 hour.

The main difference with the bin model is that the FC state does not exist, so the (practical) MFD for networks is discontinuous at the bifurcation. The bifurcation also occurs at a lower density. Phase paths associated with loading the network at different rates also behave similarly; see Figure 11. Figure 11a shows that for the free flow network, phase paths for all loading rates
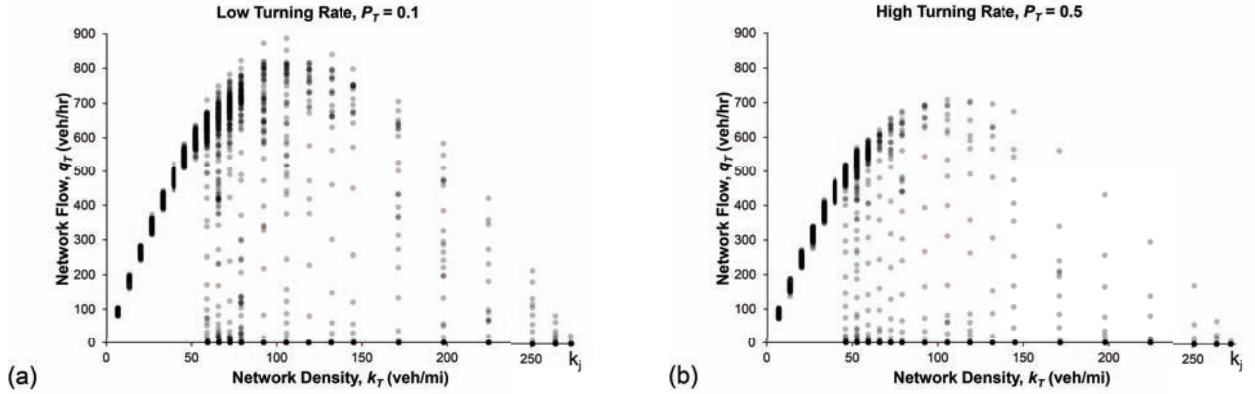
Figure 10. Simulation Flow-Density Relationship for Grid Network Showing Stability of Traffic States at Various Densities for (a) $P_T = 0.1$ and (b) $P_T = 0.5$.

follow a consistent MFD for low densities, and that these paths scatter for densities where the time to gridlock is low. Faster loading of the network allows greater flows to be observed at high network densities before the system stabilizes in gridlock. Note that consistency in the phase paths for a given loading rate does not imply stability of the traffic states. Simulations of San Francisco (Geroliminis and Daganzo, 2007) with different demand patterns (Figure 11b) also shows a consistent MFD at low densities which bifurcates at greater densities and tends to jam well before the entire network is full of vehicles (theoretical jam density is 270 veh/mi).
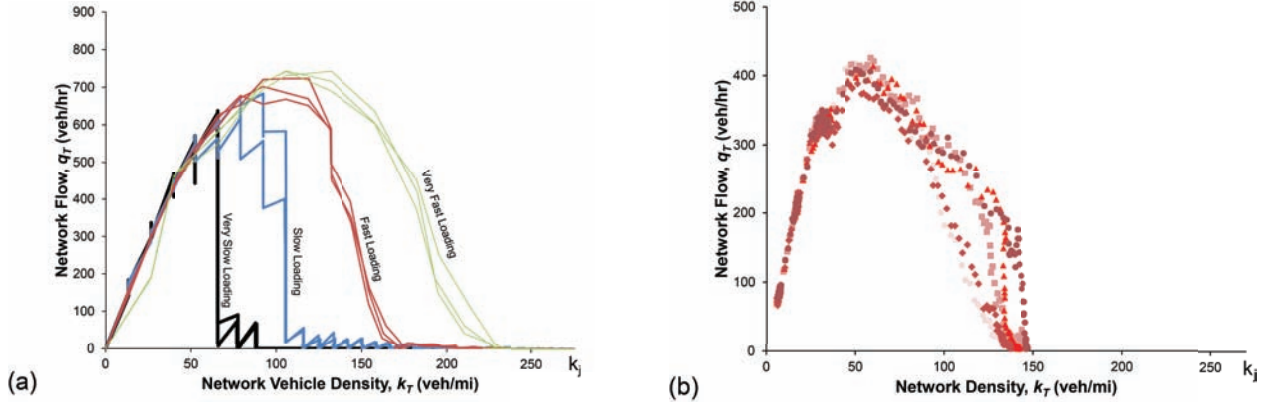

Figure 11. Simulated Phase Paths for Grid Network Showing Effect for Different Demand Rates in (a) Microsimulation of Grid Network (with $P_T = 0.5$) and (b) Microsimulation of Different Demands in San Francisco (from Geroliminis and Daganzo, 2007). In both cases $k_j = 270$ veh/mi.

5 Driver Adaptation

The results so far are a 'worst case' because they assume drivers follow rigid routes, i.e., they turn randomly without regard for traffic conditions. Therefore, it is reasonable to ask whether adaptation can eliminate or postpone the bifurcation. To answer this question systematically, driver adaptation is studied with the 2-bin model for a symmetric network. It is assumed that some proportion, α, of the drivers are 'adaptive' and will not turn from a less congested bin onto a more congested one.

This behavior can be modeled as in Section 3 using the following modified function for the flow that goes out of one bin to its companion:

$$F^*(k) = \begin{cases} (1-\alpha)F(k) & \text{if } k \leq k_T/2, \\ F(k) & \text{if } k > k_T/2. \end{cases} \tag{12}$$

Figure 12 graphically displays how F^* differs from F for the three different intersecting patterns that arise for different values of k_T when α is less than a critical value ($\alpha_c = 1 - w/v$). The three different ranges of k_T are named for reasons that will become apparent: (i) **F**ree-**F**ree/**C**ongested-**C**ongested (or FF/CC), (ii) **F**ree-**C**ongested/**C**ongested-**C**ongested (or FC/CC), and (iii) **J**am/**C**ongested-**C**ongested (or J/CC).

Note, a bifurcation occurs when k_T transitions between patterns (i) (which has a unique equilibrium) and (ii) (which does not). The reader can verify that when $\alpha > \alpha_c$, the system only exhibits two different patterns depending on k_T: **F**ree-**F**ree/**C**ongested-**C**ongested (or FF/CC) and **J**am/**C**ongested-**C**ongested (or J/CC).
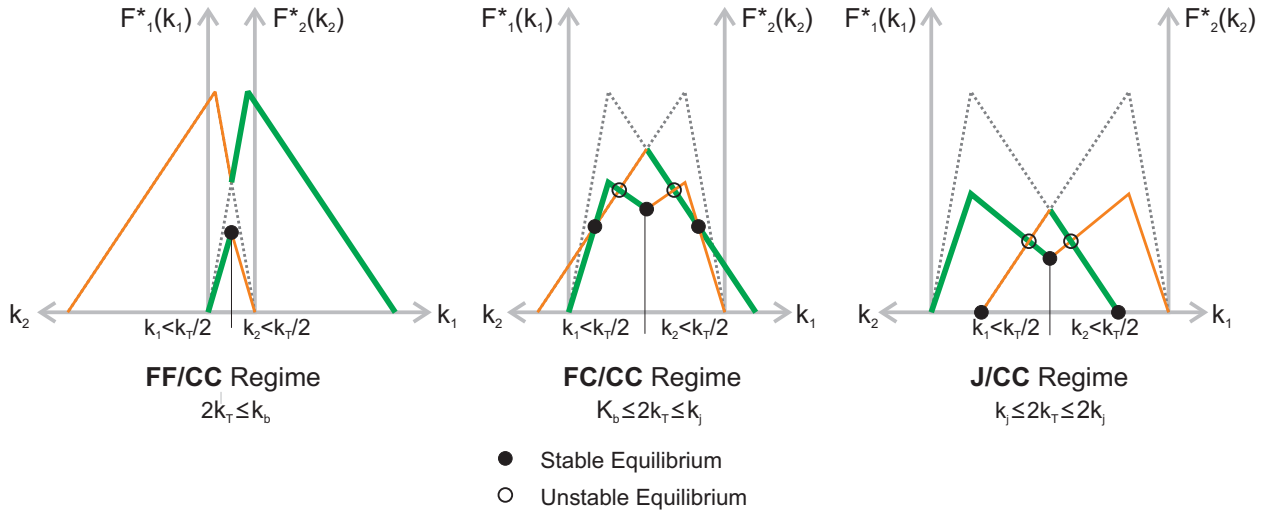

Figure 12. Change in $F(k)$ Due to Driver Adaptation for Different Regimes ($\alpha \leq 1 - w/v$): solid lines are F^*, dotted lines F.

Figure 13 presents the resulting phase diagram and MFD for the two cases. For lower adaptation levels (Figure 13a), a single stable equilibrium exists for k_T less than a bifurcation density, k_b. For greater densities, the MFD exhibits two branches. This bifurcation density increases linearly with α from $k_b = k_c$ when $\alpha = 0^+$ (negligible driver adaptation) to $k_b = k_j/2$ when $\alpha = \alpha_c$. In other words, the more adaptive drivers are, the greater the range of densities for which the MFD is single-valued; therefore, driver adaptivity increases the reproducibility of the MFD as one might expect.

For higher levels of driver adaptation (Figure 13b), the lower MFD branch disappears, but the jammed states remain. In this case, the bifurcation takes place at $k_T = k_j/2$ and multivaluedness persists for $k_T > k_j/2$.

Figure 13 also shows phase paths from simulations of the 2-bin model. These phase paths show that when the level of driver adaptation is low ($\alpha = 0.3$ in the figure) the phase paths follow the MFD up to the bifurcation, after which they are not reproducible. When driver adaptation is high ($\alpha = 0.8$ in the figure) the phase paths are reproducible for almost the entire range of densities.

For real networks where people can adapt by choosing less congested routes, we would expect to see similar patterns. The only difference should be in the location of the bifurcation on the
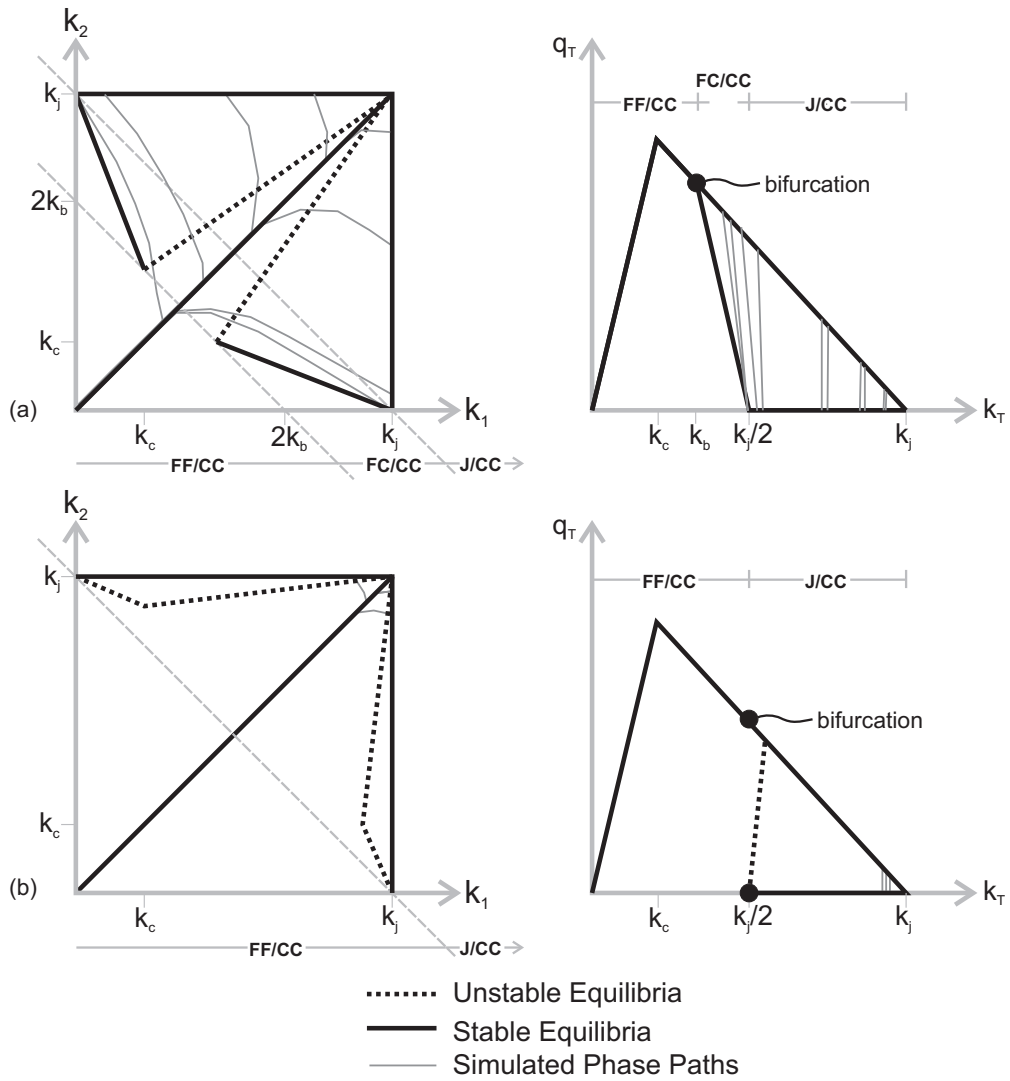
Figure 13. Phase Diagram and MFD with Phase Paths for (a) Low Levels of Driver Adaptation ($\alpha < \alpha_c$) and (b) High Levels of Driver Adaptation ($\alpha < \alpha_c$)

congested branch of the MFD. Figure 14 shows simulated data of adaptive demand in Nairobi, Kenya, and measured data from Yokohama, Japan, which support this observation. The Yokohama network appears to be more stable, and this is probably due to the fact that real drivers adapt more intelligently to traffic conditions that simulated drivers. Although traffic in Yokohama is congested during peak hours, densities large enough to see a bifurcation of the MFD were not observed. Nairobi's network, however, appears to undergo a bifurcation at network density as low as $k_T = 40$ veh/mi-lane. This network under-performs because (as explained in Gonzales et al., 2009) it lacks redundancy (which prevents drivers from shifting to nearby underused links) and flows are restricted by a few key intersections so that few vehicles are required to jam it.

The findings in this paper pertain to homogeneous, redundant networks where vehicles circulate indefinitely without exiting. Although this sheds light on some unresolved issues, the effect of exits and network heterogeneity deserve further exploration.
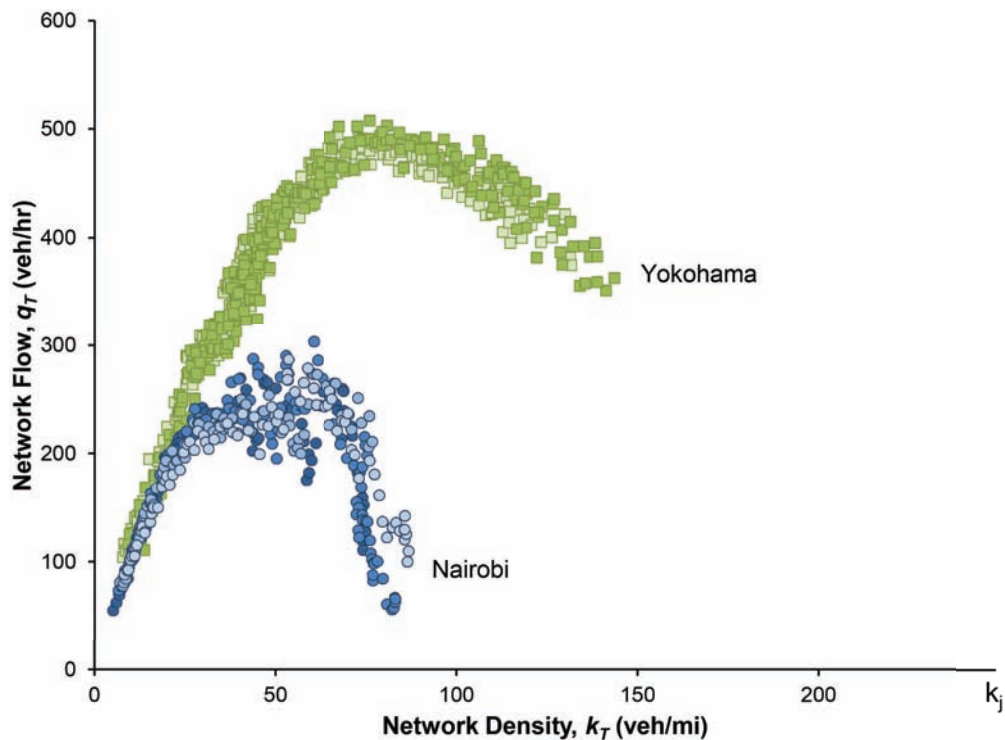

Figure 14. Comparison of Macroscopic Flow-Density Phase Paths for Nairobi (simulated; Gonzales et al., 2009) and Yokohama (measured; Geroliminis and Daganzo, 2008).

Acknowledgments

References

Daganzo, C. (1998). Queue spillovers in transportation networks with a route choice. *Transportation Science*, 32(1):3–11.

Daganzo, C. (2005). Improving city mobility through gridlock control: an approach and some ideas. *UC Berkeley, Volvo Working Paper*, UCB-ITS-VWP-2005-1:1–28.

Daganzo, C. (2006). In traffic flow, cellular automata = kinematic waves. *Transportation Research Part B: Methodological*, 40(5):396–403.

Daganzo, C. F. and Geroliminis, N. (2008). An analytical approximation for the macroscopic fundamental diagram of urban traffic. *Transportation Research Part B*, 42(9):771–781.

Edie, L. (1965). Discussion of traffic stream measurements and definitions. In *Proceedings*, page 139. Organisation for Economic Co-operation and Development.

Gayah, V. V. and Daganzo, C. (2010). Exploring the effect of turning maneuvers and route choice on a simple network. *UC Berkeley, Volvo Working Paper*.

Geroliminis, N. and Daganzo, C. F. (2007). Macroscopic modeling of traffic in cities. In *TRB 86th Annual Meeting*, number 07-0413.

Geroliminis, N. and Daganzo, C. F. (2008). Existence of urban-scale macroscopic fundamental diagrams: Some experimental findings. *Transportation Research Part B*, 42(9):759–770.

Godfrey, J. (1969). The mechanism of a road network. *Traffic Engineering and Control*, 11:323–327.

Gonzales, E., Chavis, C., Li, Y., and Daganzo, C. (2009). Multimodal transport modeling for Nairobi, Kenya: Insights and recommendations with an evidence based model. *UC Berkeley, Volvo Working Paper*.

Herman, Robert; Malakhoff, L. and Ardekani, S. (1988). Trip time-stop time studies of extreme driver behaviors. *Transportation Research Part A*, 22(6):427–433.

Herman, R. and Prigogine, I. (1979). A two-fluid approach to town traffic. *Science*, 204(4389):148–151.

Mazloumian, A., Geroliminis, N., and Helbing, D. (2009). The spatial variability of vehicle densities as determinant of urban network capacity. *Working Papers*.

Nagel, K. and Schreckenberg, M. (1992). A cellular automaton model for freeway traffic. *J. Phys. I France*, 2(12):2221–2229.